

SHINING LIGHT ON DARK MATTER

M.Sc. Thesis

By

ROHIT GUPTA



DISCIPLINE OF PHYSICS

INDIAN INSTITUTE OF TECHNOLOGY INDORE

JUNE 2015

SHINING LIGHT ON DARK MATTER

A THESIS

*Submitted in partial fulfillment of the
requirements for the award of the degree
of*
Master of Science

by

ROHIT GUPTA



DISCIPLINE OF PHYSICS
INDIAN INSTITUTE OF TECHNOLOGY INDORE
JUNE 2015



INDIAN INSTITUTE OF TECHNOLOGY INDORE

CANDIDATE'S DECLARATION

I hereby certify that the work which is being presented in the thesis entitled **SHINING LIGHT ON DARK MATTER** in the partial fulfillment of the requirements for the award of the degree of **MASTER OF SCIENCE** and submitted in the **DISCIPLINE OF PHYSICS, Indian Institute of Technology Indore**, is an authentic record of my own work carried out during the time period from July 2014 to June 2015 under the supervision of Dr. Subhendu Rakshit, Associate Professor, IIT Indore.

The matter presented in this thesis has not been submitted by me for the award of any other degree of this or any other institute.

Signature of the student with date
ROHIT GUPTA

This is to certify that the above statement made by the candidate is correct to the best of my knowledge.

Signature of the Supervisor of
M.Sc. thesis (with date)
Dr. Subhendu Rakshit

Rohit Gupta has successfully given his M.Sc. Oral Examination held on **30 June 2015..**

Signature(s) of Supervisor(s) of MSc thesis
Date:

Convener, DPGC
Date:

Signature of PSPC Member #1
Date:

Signature of PSPC Member #2
Date:

Acknowledgment

I would like to express my special thanks of gratitude to my advisor Dr. Subhendu Rakshit who gave me the opportunity to do this project and helped me a lot while doing this project.

I would also like to thank my senior Najimuddin Khan and Siddharth Karmakar for their kind support and valuable guidance.

I thank my classmates Anupriya Aggarwal, Md. Balal, Rupnayan Borah, Uttiya Sarkar and Ashish Sehwat, my seniors in physics department Shailendra Saxena, Trayambak Bhattacharyya, Sudeep Ghosh and Sudip Naskar for their help and motivation without which this work would not have been possible.

Abstract

In this report we present the basic understanding of what is dark matter and what are the evidences and detection methods for dark matter. We explain few asymmetric dark matter models that can possibly explain dark matter along with baryogenesis. We also explain multicomponent dark matter model and techniques required for constructing a model. Based on that we construct a model for two dark matter candidates.

CONTENTS

1. Introduction
2. Evidence of Dark Matter
3. Detection Method
4. Relic Density
5. Review of Asymmetric Dark Matter
6. Multicomponent Dark Matter
7. Inert Higgs Doublet Model
8. New Model
9. Imaginary term in the potential
10. Positron Excess as a ray of hope for Dark Matter Searches.
11. Gamma Ray Excess from Galactic Center
12. Experimental Results
13. Conclusion
14. References

1 Introduction

Dark Matter (DM) is one of the biggest mysteries as far as modern particle and astro-physics are concerned. It constitutes about 25% of total content of our Universe whereas the visible matter which includes all matter which we can observe by telescope working at different frequency range of electromagnetic spectrum constitutes only 5%. These densities are expressed in terms of critical density. Critical density is the density of the Universe when we consider it to be flat.

Dark Matter is mysterious because it can neither be seen by our eyes nor observed by any telescope directly, although its effect can be observed which we will discuss in subsequent sections. Its ‘invisible’ character simply means that it can neither absorb nor emit electromagnetic radiation. But it has mass so it can interact with visible matter through gravitational interaction. Based on the observation and calculation, it was also found that most of the dark matter is non-baryonic in nature. Currently most of the theories of dark matter assume it to be cold which means non-relativistic so as to explain the structure formation.

There are many prominent evidences about the existence of dark matter. The first evidence about existence of dark matter was given by Fritz Zwicky way back in 1933. He was studying motion of galaxies in a galaxy cluster called Coma cluster and used Virial theorem to determine mass in the cluster and then matched it with mass of visible matter (calculated from luminosity) in Coma cluster to show that a substantial amount of mass was invisible. Later on there were many evidences suggesting the existence of dark matter. I will discuss about them in the next section.

Dark Matter is very well accepted theory to explain excess gravity although there are few other theories that can explain discrepancies found in galactic

rotation curves. Modified Newtonian Dynamics (MOND) is one of them first proposed by Israeli physicist Mordehai Milgrom in 1983. He proposed that anomaly in rotation curve for stars in outer region of galaxy can be explained by modifying Newton's second law making force proportional to square of acceleration for object far from core of the galaxy and divide the expression by a constant so as to take care of dimension. But this theory was discarded because it was unable to explain other observations like gravitational lensing.

2 Evidence of Dark Matter

There are many evidences to support the argument that our Universe contains a large amount of matter which is invisible to us. It was first observed by Fritz Zwicky and later on by many others.

2.1 Galaxy Rotation Curve

Discrepancy observed in the galactic rotation was one of the strongest evidences of the existence of dark matter. It was observed by Vera Rubin in late 1960's. She had taken the observation of rotation of stars in our galaxy with respect to their distance from the center of the galaxy. She found that after a certain distance from the center of our galaxy, rotation speed of all stars is almost constant. But it was expected that velocity should decrease after certain distance.

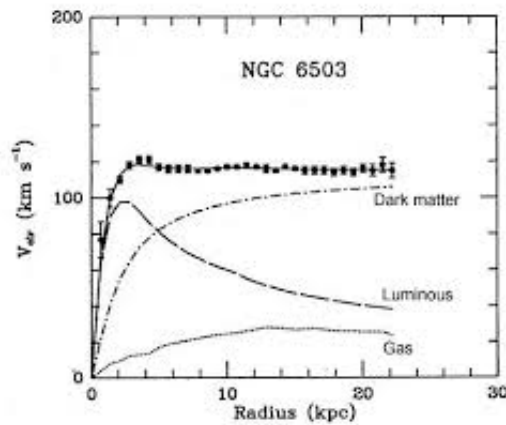


Figure 1: Galaxy rotation Curve

For regions close to center of galaxy, mass is given as

$$M_r = \frac{4\pi r^3 \rho}{3} \quad (1)$$

For a star of mass m , centripetal force is related to gravitational force as

$$\frac{mv^2}{r} = \frac{GM_r m}{r^2} \quad (2)$$

So for region close to center $v \propto r$.

But after some distance, visible mass becomes constant. So M_r is constant. Hence $v \propto r^{-1/2}$ which matches with the curve of luminous matter. But actual observation is that velocity is constant after some distance which means that $M_r \propto r$. Thus one can infer that mass is increasing with distance but luminous matter is constant. So it implies that there exists some matter in halo of our galaxy which is not luminous. So analyzing the graph in Fig. 1, Vera Rubin found that there should be a halo of dark matter around a galaxy.

2.2 Gravitational Lensing

It is an important technique to calculate mass of any massive object. As we know, light bends when it passes through a strong gravitational field due to the curvature of space-time. More is the mass, more is curvature hence more is the bending of light. Hence mass can have its imprint on the light passing through it.

But the question arises that why light will bend when it passes through a object?

As we know that gravitational force acts between two massive objects, but rest mass of photon is zero. But it is affected by the gravitational field of a massive object. Gravity can be realized as an effect arising due to the curvature of spacetime in presence of a massive object. And since light flows through the spacetime as if path itself is curved. Then anything flowing through it will bend.

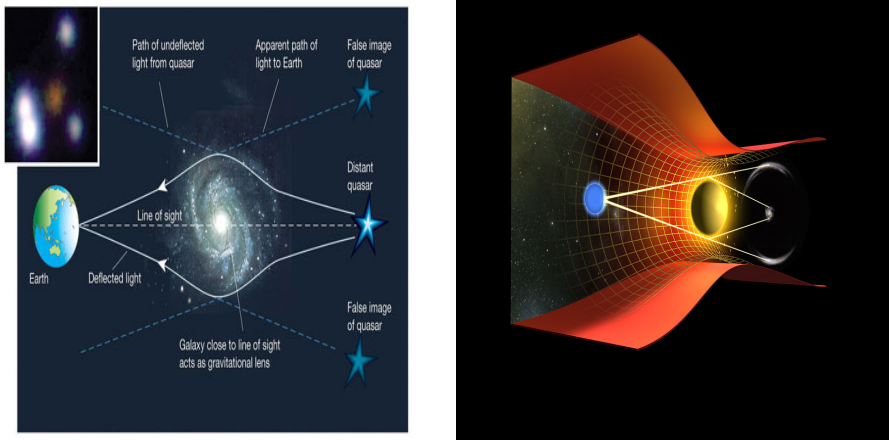


Figure 2: (a) A 2 Dimensional image of how light bends while passing through a massive object (galaxy in figure). (b) It shows how in 3 dimensions, a circle was formed due to gravitational lensing.

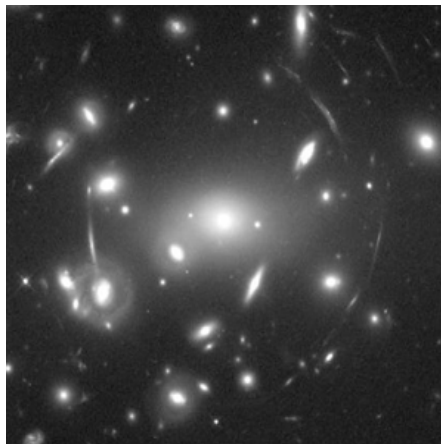


Figure 3: An image of Abell 2218 Galaxy Cluster taken by Hubble Space Telescope showing circle. Here amount of mass calculated from bending of light does not matches with amount of mass calculated from luminosity. It clearly predicts that there is some mass which is not luminous.

2.3 Other Evidences

There are few other observations that suggest the existence of dark matter. Cosmological parameters determined from power spectrum of cosmic mi-

microwave background (CMB) anisotropy also point towards a significant amount of non-baryonic matter. Density parameter of any particular component is given as the ratio of energy density of that particular component with respect to total energy density (critical density) of our Universe. Since density parameter of all matter in the Universe is $\Omega_M h^2 = 0.127_{-0.013}^{+0.007}$ while density parameter of all baryonic matter is $\Omega_B h^2 = 0.0223_{-0.0009}^{+0.0007}$, thus a significant amount of matter about $\Omega_{NB} h^2 = 0.105_{-0.013}^{+0.007}$ is non-baryonic in nature. Observation of Bullet cluster also supports the existence of dark matter. Bullet cluster consists of galaxy clusters undergoing merger with each other.



Figure 4: *An artistic image made by mixing observation from Chandra X-Ray Observatory and Gravitational Lensing.*

Pink region is the visible baryonic matter while blue region is dark matter. As we can see that baryonic matter gets concentrated. Electromagnetic interactions between baryonic matter causes them to concentrate near point of impact. But shape of dark matter cloud (blue region) does not change since we know that they do not undergo electromagnetic interaction.

3 Detection Methods

There are some detection methods through which we can detect the presence of dark matter directly or indirectly.

3.1 Direct Detection

One of the most widely accepted candidates for dark matter is Weakly Interacting Massive Particle (WIMP). Since our galaxy has a halo of dark matter and our solar system is moving in the galaxy, so there is a flux of dark matter passing through us regularly.

Direct Detection experiments are designed to detect the elastic scattering of WIMP dark matter from a target nucleus. Since they are very weakly interacting, they can easily pass through wall, rock etc. Detectors are placed deep inside rock so that background can be minimized. Since dark matter particles are weakly interacting so they can go deep inside the rock but normal baryonic matter cannot go that much deep.

Basic mechanism of all direct detection experiments is as follows:

When a dark matter particle arrives at the detector, it may undergo elastic scattering with the nucleus and deposits some of its energy. This leads to rise in temperature which we can detect using cryogenic detector working in millikelvin range. In some cases, such collisions lead to generation of flash which can also be detected using noble liquid detector.

There are few cryogenic detectors like CRESST at Gran Sasso National laboratory Italy, CDMS at Stanford University etc. Noble liquid detectors include XENON at Gran Sasso Italy, Particle and Astrophysical Detector (PandaX) at China etc.

3.2 Indirect Detection

Indirect detection method is another method for detection of dark matter. Since dark matter also have particles and anti-particles so they can annihilate to form standard model particles like electron, positron, gamma ray etc. Also if WIMP is unstable it may decay to standard model particle. So, in indirect detection experiment we search for excess of standard model particles.

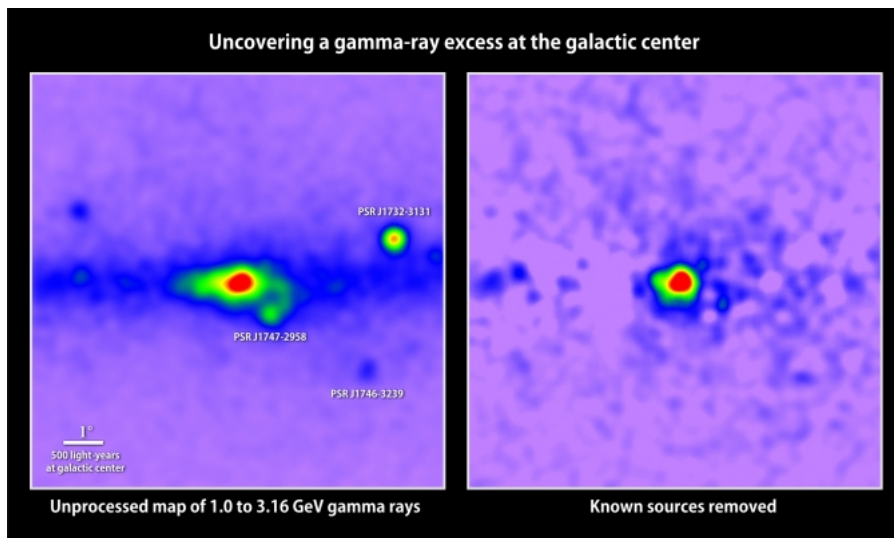


Figure 5: *This figure shows excess of gamma ray found at the galactic center of our Milky Way by Fermi Gamma Ray Telescope.*

From Fig. 5 it is quite evident that even after all known sources were removed, still substantial amount of gamma ray was present. Physicists suggested that this was formed due to the annihilation of dark matter at galactic center since high gravitational field at the galactic center might have trapped dark matter and caused their annihilation.

Alpha Magnetic Spectrometer (AMS) is an instrument installed at International Space Station. It detects excess of positron produced from annihilation of dark matter in some energy range. PAMELA also searches for

excess positron. Fermi Gamma-ray Space Telescope (FGST) detects excess of gamma ray emission. In particular, it has detected the excess of gamma ray at galactic center.

4 Relic Density

Boltzmann equation relates rate of change of number density of a particle to its annihilation and equilibrium number density. Since after particle decouples from thermal bath, it gets freezed out and hence its annihilation cross section becomes negligible. So we can calculate relic density using Boltzmann equations. It also contain scale factor which takes care of expansion of the Universe. Let's consider a process $\chi_1\chi_2 \leftrightarrow \chi_3\chi_4$ where χ_i are some elementary particles. Then Boltzmann equation for time evolution of number density n_1 of χ_1 is given as^[1]

$$a^{-3}\frac{d(n_1a^3)}{dt} = \langle\sigma v\rangle n_1^0 n_2^0 \left(\frac{n_3 n_4}{n_3^0 n_4^0} - \frac{n_1 n_2}{n_1^0 n_2^0} \right). \quad (3)$$

where n_i^0 are number density in thermal equilibrium. Here $\langle\sigma v\rangle$ is thermal averaged annihilation cross section.

For the present case consider n_3 and n_4 are non-interacting particles, so $n_{3,4} = n_{3,4}^0$ and $n_1 = n_2 = n_\chi$. Then Boltzmann equation becomes

$$a^{-3}\frac{dn_\chi a^3}{dt} = \langle\sigma_{ann}v\rangle [(n_\chi^0)^2 - (n_\chi)^2]. \quad (4)$$

Now in order to simplify this equation, consider

$$Y = \frac{n_\chi}{s}, \quad (5)$$

where s is entropy density and given as

$$s = g_* T^3 \left(\frac{2\pi^2}{45} \right)^{1/2}. \quad (6)$$

Consider Friedmann equation for $k = 0$

$$\left(\frac{\dot{a}}{a} \right)^2 = \frac{8\pi G\rho}{3}. \quad (7)$$

From statistical mechanics we know that energy density ρ is given in terms of energy $E(p)$ and distribution function $f(p)$ as

$$\rho = \frac{g}{(2\pi)^3} \int E(p) f(p) d^3p, \quad (8)$$

for Bose gas

$$f(p) = \frac{1}{\exp(\frac{E(p)}{T}) + 1}, \quad (9)$$

So

$$\rho = \frac{g}{(2\pi)^3} \int \frac{E(p)}{\exp(\frac{E(p)}{T}) + 1} 4\pi p^2 dp. \quad (10)$$

For relativistic case, $E(p) = \frac{p^2}{2m}$ so

$$\rho = \frac{\pi^2}{30} g T^4, \quad (11)$$

Hence, from (7)

$$H^2 = \frac{g\pi^2 T^4}{90 M_{pl}^2}, \quad (12)$$

$$M_{pl} = \sqrt{\frac{\hbar c}{8\pi G}}. \quad (13)$$

We had started with relativistic case when temperature $T > m_\chi$ but after some time temperature drops below m_χ and then χ becomes non-relativistic. For non-relativistic case we can consider classical Maxwell Boltzmann distribution. So equilibrium number density is given as

$$n_\chi^0 = \int \frac{d^3p}{(2\pi)^3} e^{-E/T} \quad \left(E = m_\chi + \frac{\vec{p}^2}{2m_\chi} \right) \quad (14)$$

On solving it, we get

$$n_\chi^0 = e^{-x} \frac{m_\chi^3}{(2\pi x)^{3/2}} \quad (15)$$

Where $x = \frac{m_\chi}{T}$

So

$$Y_0 = \frac{n_\chi^0}{s} = \frac{45}{g_* 2\pi^2} \left(\frac{x}{2\pi}\right)^{\frac{3}{2}} e^{-x}, \quad (16)$$

$$Y_0 = 0.145 x^{\frac{3}{2}} e^{-x}, \quad (17)$$

Here

$$g_* = 1. \quad (18)$$

where g_* is number of spin states.

Now changing the variable from n_χ to Y , Boltzmann equation becomes

$$\frac{dY}{dx} = -\frac{1}{x^2} \frac{s(m_\chi)}{H(m_\chi)} \langle \sigma v \rangle (Y^2 - Y_0^2). \quad (19)$$

Proof:

Since

$$T = \frac{m_\chi}{x}, \quad (20)$$

and $s \propto T^3$, so we can write

$$s(T) = \frac{s(m_\chi)}{x^3}. \quad (21)$$

Also since $H \propto T^2$, so

$$H(T) = \frac{H(m_\chi)}{x^2}, \quad (22)$$

From (12) for relativistic case

$$H = \sqrt{\frac{g\pi^2 T^4}{90 M_{pl}^2}}, \quad (23)$$

And as we know for relativistic (radiation dominated) case

$$H = \frac{1}{2t}, \quad (24)$$

Comparing (23) and (24)

$$dt = -\frac{m_\chi^2}{H(m_\chi)T^3}dT. \quad (25)$$

But

$$x = \frac{m_\chi}{T}, \quad (26)$$

So

$$dT = -\frac{T^2}{m_\chi}dx, \quad (27)$$

Hence

$$dt = x\frac{dx}{H(m_\chi)}, \quad (28)$$

Putting (5), (21) and (22) in (19)

$$\frac{dY}{dx} = -\frac{1}{x^2}\frac{s(T)x^3}{H(T)x^2}\langle\sigma v\rangle\frac{(n_\chi^2 - n_\chi^{02})}{s^2(T)}, \quad (29)$$

On solving it using (28) we get

$$\frac{dn_\chi}{dt} + 3n_\chi H = \langle\sigma_{ann}v\rangle[(n_\chi^0)^2 - (n_\chi)^2]. \quad (30)$$

The above expression can be reduced to equation (4) since

$$H = \frac{\dot{a}}{a}, \quad (31)$$

Here

$$\frac{s(m_\chi)}{H(m_\chi)} = \frac{2\pi^2}{45}\sqrt{\frac{90}{\pi^2}}\sqrt{g_*}m_\chi M_{pl} = 1.32\sqrt{g_*}m_\chi M_{pl}. \quad (32)$$

Once particle is non-relativistic ($T \ll m_\chi$) then annihilation cross section is insensitive of temperature

So

$$\frac{s(m_\chi)}{H(m_\chi)}\langle\sigma v\rangle \quad (33)$$

is just a number.

So we can write

$$y = \frac{s(m_\chi)}{H(m_\chi)}\langle\sigma v\rangle Y \quad (34)$$

So we can further simplify our Boltzmann equation as

$$\frac{dy}{dx} = -\frac{1}{x^2}(y^2 - y_0^2) \quad (35)$$

So we have a equation which relates mass, annihilation cross section, number density and equilibrium number density. We can solve it using analytic approximation or numerical integration to get relic abundance if mass and annihilation cross section are provided. Also since

$$Y_0 = \frac{n_\chi^0}{s} \quad \text{and} \quad n_\chi^0 = \frac{\rho_\chi}{m_\chi} \quad (36)$$

So

$$\Omega_\chi h^2 = h^2 \frac{\rho_\chi}{\rho_{critical}} = \frac{h^2 m_\chi s Y_0}{\rho_{critical}} \quad (37)$$

Hence, we can get density parameter for given dark matter mass and equilibrium number density.

5 Review of Asymmetric Dark Matter

Asymmetric Dark Matter (ADM) model is the model where we study the correspondence between dark sector and visible sector, for example, we propose some dark electron, dark photon etc.

The main motivation behind ADM is the similarity between cosmological density parameter of visible matter and dark matter^[2]

$$\Omega_{DM} \simeq 5\Omega_{VM} \quad (38)$$

Such similarity suggests that there must be some connection between origin and cosmological evolution of visible matter and dark matter.

As we know, at present our Universe contains only visible matter and no visible antimatter because some asymmetry between matter and anti matter had originated in early Universe and so the symmetric part of visible matter had annihilated and we are left with only matter. ADM model suggests similar mechanism for dark sector i.e. in dark sector we also had asymmetry between matter and antimatter and symmetric part got annihilated.

In most of the ADM model, number density of dark matter is same as number density of visible matter. So, from the above relation its mass may lie in 1-15 GeV range. Also, there are strong evidences for dark matter in this mass range by DAMA^[3], CoGENT^{[4],[5]}, CRESST^[6] and CDMS^[7] experiments. All of them are direct detection experiments.

Since ADM model tries to make connection between visible matter and dark matter, so we have to assume that dark matter must also be stabilized by some dark gauge symmetry groups. These groups can have some dark quantum numbers which are broken so as to explain asymmetry.

Since in visible sector we have some particles that are stable due to some constraints like electron is stable because it is the lightest charged particle.

Similarly, proton is the lightest baryon. Also simultaneous existence of stable electron and proton is responsible for making Universe to be neutral. So, similarly in dark sector we must have some particles stabilized due to conservation of some quantum numbers.

Now let us concentrate on baryon number conservation since it is the most important requirement for mass as proton is stabilized by baryon number. Moreover early Universe mainly contains proton and electron but proton is very massive compared to electron.

5.1 Sakharov Conditions

As we know that there is baryon asymmetry in the Universe. But we cannot say that such asymmetry was there since the beginning of Universe since inflation must have washed out any such asymmetry. So our early Universe must be baryon symmetric. In 1967 Andrei Sakharov proposed the conditions required for generation of baryon asymmetry of the Universe. He proposed three conditions required for origin of asymmetry from baryon symmetric Universe:

1. Existence of baryon number violation.

As we can see that our Universe mainly consists of baryons and a very trace amount of antibaryons. So, some process must have happened in the due course of time so that all the antimatter got washed out.

2. Existence of CP violation.

C symmetry will also be violated. Since, if not, then process which produces more baryons than antibaryons will be counter balanced by its charge conjugate which produce more antibaryons than baryons.

3. Baryon number violating processes out of equilibrium.

This criterion suggests that the reaction responsible for creating asym-

metry between production of baryons and antibaryons must be occurring at a rate smaller than the expansion rate of the Universe so that created asymmetry would not have washed out due to annihilation.

5.2 Asymmetry Generation Mechanism

5.2.1 Out-of-equilibrium decay:

The basic idea behind this mechanism is that there was a massive unstable particle. After it decouples from thermal plasma, it started decaying. The interactions that are responsible for its decay also violates baryon number and CP. So decay rate of particle and its antiparticle was different and hence created asymmetry, and since this was out of equilibrium decay so asymmetry cannot get washed out by inverse decay.

5.2.2 Asymmetric freeze out:

Self-annihilation of dark matter with dark antimatter is required for annihilation of symmetric part which is mandatory in ADM model. But dark matter can also have baryon number violating co-annihilation with standard model (SM) species. Since dark matter and dark antimatter co-annihilation rates can be different and if co-annihilation rates start dominating over self-annihilation rates then they will decouple at different temperature and hence have different relic density.

5.3 Dark Interaction

The important feature of ADM models is the efficient annihilation of symmetric part of DM in the early Universe. It can have a dark gauge force $U(1)_D$ under which all dark matter and dark antimatter particles have charge. Dark

Matter charged under $U(1)_D$ can annihilate to give dark photons that can be massless or massive, also dark matter can annihilate via dark photon to other lighter species charged under $U(1)_D$. If dark photon is massless, it will act as extra radiation during decoupling of CMB. Also, within observational errors, there is tantalizing evidence for existence of quite a significant amount of extra radiation in both primordial element abundance measurement and CMB anisotropy results from WMAP^[8] and Planck^[9].

5.4 Asymmetric Dark Matter Model

Now we study briefly about few asymmetric dark matter models:

5.4.1 Exciting Dark Matter: A novel mechanism to explain 511 keV line observed at galactic center

A gamma ray excess at 511 keV was found at galactic center which matches with the positronium emission line but there is no obvious astrophysical source that can explain such excess. But the mechanism of excited state of dark matter can explain this excess. If WIMP has something analogous to excited states^[10] then inelastic scattering between them leads to their transition to some excited state. If energy gap between these two states is more than $2m_e$ (here m_e is mass of electron) then their decay could lead to emission of electron-positron pair.

6 Multicomponent Dark Matter

6.1 Introduction

Multicomponent dark matter model consists of models where we have more than one dark matter candidate with all of them stable under given symmetries and satisfy relic abundance observation. In multicomponent case we can have more diverse annihilation and co-annihilation processes and we can explain different observations that require different mass regime of dark matter.

There are many observational evidences that suggests dark matter in completely different mass range. Indirect detection experiment like PAMELA has reported excess of cosmic ray positron suggesting the mass range of around 10-100 GeV. There are some other indirect detection experiments like HEAT and AMS that agree with constraint put by PAMELA on mass range of dark matter. Fermi's result also suggests mass range of 100-200 GeV. However DAMA which is a direct detection experiment suggests a mass range of 3-10 GeV.

In most of the multicomponent model, dark matter is stabilized by discrete symmetries. Discrete symmetry means that it can have only few defined possible values. The simplest example of discrete symmetry is R -parity of supersymmetry under which each superpartner is assigned $R = -1$ and ordinary partners have $R = 1$.

In general a field ϕ transforms under a general discrete symmetry Z_N as

$$\phi \rightarrow \exp\left(\frac{2\pi i}{N}\right) \phi \quad (39)$$

Also a more interesting feature of discrete symmetry is that lightest particle charged under this symmetry is stable and hence could be a dark matter.

6.2 Techniques used for constructing a model

For constructing any model we first have to decide its field content and the symmetry under which we want our potential to be invariant. We have to decide our field content and symmetry on the basis of what are the interaction terms which we want in our potential and in our relic density calculation.

Let us review a simple model^[11] consisting of two singlet scalars S, S' along with standard model particles, where S is stabilized by Z_2 and S' is stabilized by Z'_2 . Z_2 and Z'_2 are different in the sense that they are symmetry groups in different space. The general potential without considering any symmetry is

$$\begin{aligned}
V(H, S, S') = & \frac{m^2}{2} H^\dagger H + \frac{\lambda}{4} (H^\dagger H)^2 \\
& + \frac{\delta_1}{2} H^\dagger H S + \frac{\delta_2}{2} H^\dagger H S^2 + \frac{\delta_1 m^2}{2\lambda} S + \frac{k_2}{2} S^2 + \frac{k_3}{3} S^3 + \frac{k_4}{4} S^4 \\
& + \frac{\delta'_1}{2} H^\dagger H S' + \frac{\delta'_2}{2} H^\dagger H S'^2 + \frac{\delta'_1 m^2}{2\lambda} S' + \frac{k'_2}{2} S'^2 + \frac{k'_3}{3} S'^3 + \frac{k'_4}{4} S'^4 \\
& + \frac{\delta''_2}{2} H^\dagger H S' S + \frac{k''_2}{2} S S' + \frac{1}{3} (k_3^a S S S' + k_3^b S S' S') \\
& + \frac{1}{4} (k_4^a S S S' S' + k_4^b S S S S' + k_4^c S S' S' S')
\end{aligned} \tag{40}$$

The transformation of field S and S' are given as

$$S \xrightarrow{Z_2} -S \quad \text{and} \quad S' \xrightarrow{Z'_2} -S' , \tag{41}$$

Under these transformations with S, S' and Higgs H , potential invariant under $Z_2 \times Z'_2$ is given by

$$\begin{aligned}
V(H, S, S') = & \frac{m^2}{2} H^\dagger H + \frac{\lambda}{4} (H^\dagger H)^2 \\
& + \frac{\delta_2}{2} H^\dagger H S^2 + \frac{k_2}{2} S^2 + \frac{k_4}{4} S^4 \\
& + \frac{\delta'_2}{2} H^\dagger H S'^2 + \frac{k'_2}{2} S'^2 + \frac{k'_4}{4} S'^4 \\
& + \frac{1}{4} k_4^a S S S' S' .
\end{aligned} \tag{42}$$

We can also calculate mass term for given field S, S' using the concept of Klein-Gordon equation

$$L = \frac{1}{2}(\partial_\mu\phi)(\partial^\mu\phi) - \frac{1}{2}m^2\phi^2 = T - V \quad (43)$$

where mass term is $\frac{1}{2}m^2\phi^2$. Here, m is mass, so if we differentiate it twice with respect to ϕ , we get mass. So in similar way, for calculating mass of any field in a given potential, we have to separate field square terms and then do double differentiation with respect to field.

So using similar procedure we can calculate mass of field S and S' .

$$M_S^2 = k_2 + \frac{\delta_2 v^2}{2} \quad (44)$$

$$M_{S'}^2 = k'_2 + \frac{\delta'_2 v^2}{2} \quad (45)$$

6.3 Copositivity Criteria

It is an important way to calculate condition required to ensure boundedness of scalar potential and hence to calculate vacuum stability condition. Electroweak scalar potential is bounded from below if and only if Higgs quartic coupling, λ_h , is positive. Since at higher value of ϕ , only ϕ^4 (quartic) term dominates. Hence if λ_h is negative then potential is not bounded from below and so infinite amount of energy is emitted by the field hence $\lambda_h \geq 0$

. Suppose we have a quadratic equation^[12]

$$x^T A_1 x = x_1^2 + 2x_2^2 + 3x_3^2 - 2x_1x_2 - 2x_1x_3 - 4x_2x_3,$$

Then its corresponding symmetric matrix of order 3 in (x_1, x_2, x_3) basis is given as

$$A_1 = \begin{pmatrix} 1 & -1 & -1 \\ -1 & 2 & -2 \\ -1 & -2 & 3 \end{pmatrix}$$

Similarly we can write any potential in this form. Copositivity criteria

says that a symmetric matrix A is copositive if and only if quadratic form $x^T Ax \geq 0$ for all $x \geq 0$ in non-negative orthant (quadrant in two dimensional plane). So, we can easily see that if $V = x^T Ax \geq 0$ then it must be bounded from below.

Principal submatrix of a matrix A can be obtained by deleting rows and columns of A in a symmetric way i.e. if $i_1 \dots i_k$ rows are deleted then $i_1 \dots i_k$ number of columns are also deleted. So, condition for copositivity is that determinant of positive submatrices must always be non-negative.

Hence, if matrix of a potential is copositive then it must be bounded from below. So condition for boundedness is same as condition for copositivity.

So for any general symmetric matrix of order n , it is copositive if these conditions are satisfied^[12]:

$$\lambda_{ii} \geq 0, \quad \lambda_{ij} + \sqrt{\lambda_{ii}\lambda_{jj}} \geq 0, \\ \sqrt{\prod_{i=1,2..n} \lambda_{ii}} + \sum_{i,j,k} \lambda_{ij} \sqrt{\lambda_{kk}} + \sqrt{2 \prod_{i,j,k} (\lambda_{ij} + \sqrt{\lambda_{ii}\lambda_{jj}})} \geq 0 \quad (46)$$

These conditions are called vacuum stability conditions for a given potential.

7 Inert Higgs Doublet Model

This model consists of one or two inert doublets along with a standard model Higgs where inert doublets are stabilized by some discrete symmetries like Z_2 , Z_3 etc or some combination of them like $Z_2 \times Z_3$ etc. These symmetries are preserved even after electroweak symmetry breaking. Among this inert doublet, lightest neutral one could be the possible dark matter candidate. Inert is used for the doublet since it does not couple to fermions and gauge bosons as it does not have any gauge charges.

Among these, one inert doublet plus one Higgs doublet is widely studied model, which is stabilized under a given discrete symmetry like Z_2 , where inert doublet is Z_2 odd and Higgs is Z_2 even. Z_2 odd means field transforms under Z_2 whereas even means field does not transform i.e.

$$\phi_1 \rightarrow \exp\left(\frac{2\pi i}{2}\right) \phi_1 \quad (47)$$

$$H \rightarrow H \quad (48)$$

Among the components of this inert doublet, lightest neutral field is our dark matter candidate. However if we consider two inert doublet plus one Higgs doublet case then we can have more diverse phenomenology. We can have more annihilation processes and decay processes. If lightest component of both inert doublets are stable then they can be the suitable dark matter candidates.

8 New Model

As we have already discussed, two inert doublets plus one Higgs doublet is not much explored. So here, we have done some model building with $Z_2 \times Z'_2$ symmetry.

Here our field content is ϕ_1, ϕ_2, ϕ_3 where ϕ_1 is our standard model Higgs and ϕ_2, ϕ_3 are two inert scalar doublets.

8.1 Potential

$$\begin{aligned}
V = & \mu_1^2(\phi_1^\dagger\phi_1) + \mu_2^2(\phi_2^\dagger\phi_2) + \mu_3^2(\phi_3^\dagger\phi_3) \\
& + \frac{\lambda_1}{2}(\phi_1^\dagger\phi_1)^2 + \frac{\lambda_2}{2}(\phi_2^\dagger\phi_2)^2 + \frac{\lambda_3}{2}(\phi_3^\dagger\phi_3)^2 + \lambda_4(\phi_1^\dagger\phi_1)(\phi_2^\dagger\phi_2) \\
& + \lambda_5(\phi_1^\dagger\phi_2)(\phi_2^\dagger\phi_1) + \frac{\lambda_6}{2}[(\phi_1^\dagger\phi_2)^2 + (\phi_2^\dagger\phi_1)^2] + \lambda_7(\phi_1^\dagger\phi_1)(\phi_3^\dagger\phi_3) \\
& + \lambda_8(\phi_1^\dagger\phi_3)(\phi_3^\dagger\phi_1) + \frac{\lambda_9}{2}[(\phi_1^\dagger\phi_3)^2 + (\phi_3^\dagger\phi_1)^2] + \lambda_{10}(\phi_2^\dagger\phi_2)(\phi_3^\dagger\phi_3) \\
& + \lambda_{11}(\phi_2^\dagger\phi_3)(\phi_3^\dagger\phi_2) + \frac{\lambda_{11}}{2}[(\phi_2^\dagger\phi_3)^2 + (\phi_3^\dagger\phi_2)^2] \tag{49}
\end{aligned}$$

where

$$\phi_1 = \begin{pmatrix} 0 \\ \frac{v+h}{\sqrt{2}} \end{pmatrix}, \quad \phi_2 = \begin{pmatrix} H_2^+ \\ \frac{H_{20}+iA_{20}}{\sqrt{2}} \end{pmatrix}, \quad \phi_3 = \begin{pmatrix} H_3^+ \\ \frac{H_{30}+iA_{30}}{\sqrt{2}} \end{pmatrix} \tag{50}$$

8.2 Mass Term

Using the methods in previous section we can calculate mass of neutral fields

$$m_{H_{20}}^2 = \mu_2^2 + \frac{\lambda_4 v^2}{2} + \frac{\lambda_5 v^2}{2} + \frac{\lambda_6 v^2}{2} \tag{51}$$

$$m_{A_{20}}^2 = \mu_2^2 + \frac{\lambda_4 v^2}{2} + \frac{\lambda_5 v^2}{2} - \frac{\lambda_6 v^2}{2} \quad (52)$$

$$m_{H_{30}}^2 = \mu_3^2 + \frac{\lambda_7 v^2}{2} + \frac{\lambda_8 v^2}{2} + \frac{\lambda_9 v^2}{2} \quad (53)$$

$$m_{A_{30}}^2 = \mu_3^2 + \frac{\lambda_7 v^2}{2} + \frac{\lambda_8 v^2}{2} - \frac{\lambda_9 v^2}{2} \quad (54)$$

8.3 Copositivity criteria

We can calculate boundedness of potential using equation (45)

$$\lambda_1 \geq 0, \lambda_2 \geq 0, \lambda_3 \geq 0 \quad (55)$$

$$\frac{\lambda_4 + \lambda_5 - \lambda_6}{4} + \sqrt{\frac{\lambda_1 \lambda_2}{64}} \geq 0 \quad (56)$$

$$\frac{\lambda_7 + \lambda_8 - \lambda_9}{4} + \sqrt{\frac{\lambda_1 \lambda_3}{64}} \geq 0 \quad (57)$$

$$\frac{\lambda_4 + \lambda_5 + \lambda_6}{4} + \sqrt{\frac{\lambda_1 \lambda_2}{64}} \geq 0 \quad (58)$$

$$\frac{\lambda_7 + \lambda_8 + \lambda_9}{4} + \sqrt{\frac{\lambda_1 \lambda_3}{64}} \geq 0 \quad (59)$$

$$\frac{\lambda_4}{2} + \sqrt{\frac{\lambda_1 \lambda_2}{16}} \geq 0 \quad (60)$$

$$\frac{\lambda_7}{2} + \sqrt{\frac{\lambda_1 \lambda_3}{16}} \geq 0 \quad (61)$$

$$\frac{\lambda_{10} + 2\lambda_{11}}{4} + \sqrt{\frac{\lambda_2 \lambda_3}{64}} \geq 0 \quad (62)$$

$$\frac{\lambda_{10}}{4} + \sqrt{\frac{\lambda_2 \lambda_3}{64}} \geq 0 \quad (63)$$

$$\frac{\lambda_{10}}{2} + \sqrt{\frac{\lambda_3(\lambda_{10} + \lambda_{11})}{8}} \geq 0 \quad (64)$$

$$\lambda_{10} + \lambda_{11} + \sqrt{\frac{\lambda_2 \lambda_3}{4}} \geq 0 \quad (65)$$

9 Imaginary term in the potential

When we take a closer look at the potential we can see that coefficients of last two terms are same. It has been taken deliberately in order to remove imaginary term coming in the potential as explained below.

Let us take the coefficients of last two terms to be different. So, the potential will be

$$\begin{aligned}
V = & \mu_1^2(\phi_1^\dagger\phi_1) + \mu_2^2(\phi_2^\dagger\phi_2) + \mu_3^2(\phi_3^\dagger\phi_3) \\
& + \frac{\lambda_1}{2}(\phi_1^\dagger\phi_1)^2 + \frac{\lambda_2}{2}(\phi_2^\dagger\phi_2)^2 + \frac{\lambda_3}{2}(\phi_3^\dagger\phi_3)^2 + \lambda_4(\phi_1^\dagger\phi_1)(\phi_2^\dagger\phi_2) \\
& + \lambda_5(\phi_1^\dagger\phi_2)(\phi_2^\dagger\phi_1) + \frac{\lambda_6}{2}[(\phi_1^\dagger\phi_2)^2 + (\phi_2^\dagger\phi_1)^2] + \lambda_7(\phi_1^\dagger\phi_1)(\phi_3^\dagger\phi_3) \\
& + \lambda_8(\phi_1^\dagger\phi_3)(\phi_3^\dagger\phi_1) + \frac{\lambda_9}{2}[(\phi_1^\dagger\phi_3)^2 + (\phi_3^\dagger\phi_1)^2] + \lambda_{10}(\phi_2^\dagger\phi_2)(\phi_3^\dagger\phi_3) \\
& + \lambda_{11}(\phi_2^\dagger\phi_3)(\phi_3^\dagger\phi_2) + \frac{\lambda_{12}}{2}[(\phi_2^\dagger\phi_3)^2 + (\phi_3^\dagger\phi_2)^2] \tag{66}
\end{aligned}$$

Also,

$$\phi_1 = \begin{pmatrix} 0 \\ \frac{v+h}{\sqrt{2}} \end{pmatrix}, \phi_2 = \begin{pmatrix} H_2^+ \\ \frac{H_{20}+iA_{20}}{\sqrt{2}} \end{pmatrix}, \phi_3 = \begin{pmatrix} H_3^+ \\ \frac{H_{30}+iA_{30}}{\sqrt{2}} \end{pmatrix}$$

On expanding above potential by putting all the components we get the extended version of this potential.

$$\begin{aligned}
V = & \frac{\lambda_1}{8} + \frac{\mu_1^2 h^2}{2} + \frac{\lambda_1 v h^3}{2} + \mu_1^2 h v + \frac{3\lambda_1 h^2 v^2}{4} + \frac{\mu_1^2 v^2}{2} + \frac{\lambda_1 h v^3}{2} + \frac{\lambda_1 v^4}{8} + \frac{\lambda_4 h^2 A_{20}^2}{4} \\
& + \frac{\lambda_5 h^2 A_{20}^2}{4} - \frac{\lambda_6 h^2 A_{20}^2}{4} + \frac{\mu_2^2 A_{20}^2}{2} + \frac{\lambda_4 h v A_{20}^2}{2} + \frac{\lambda_5 h v A_{20}^2}{2} - \frac{\lambda_4 h v A_{20}^2}{2} \\
& + \frac{\lambda_4 v^2 A_{20}^2}{4} + \frac{\lambda_5 v^2 A_{20}^2}{4} - \frac{\lambda_6 v^2 A_{20}^2}{4} + \frac{\lambda_2 A_{20}^4}{8} + \frac{\lambda_7 h^2 A_{30}^2}{4} + \frac{\lambda_8 h^2 A_{30}^2}{4} \\
& - \frac{\lambda_9 h^2 A_{30}^2}{4} + \frac{\mu_3^2 A_{30}^2}{2} + \frac{\lambda_7 h v A_{30}^2}{2} + \frac{\lambda_8 h v A_{30}^2}{2} - \frac{\lambda_9 h v A_{30}^2}{2} + \frac{\lambda_7 v^2 A_{30}^2}{4} \\
& + \frac{\lambda_8 v^2 A_{30}^2}{4} - \frac{\lambda_9 v^2 A_{30}^2}{4} + \frac{\lambda_{10} A_{20}^2 A_{30}^2}{4} + \frac{\lambda_{11} A_{20}^2 A_{30}^2}{4} + \frac{\lambda_{12} A_{20}^2 A_{30}^2}{4} + \frac{\lambda_3 A_{30}^4}{8} \\
& + \frac{\lambda_4 h^2 H_{20}^2}{4} + \frac{\lambda_5 h^2 H_{20}^2}{4} + \frac{\lambda_6 h^2 H_{20}^2}{4} + \frac{\mu_2^2 H_{20}^2}{2} + \frac{\lambda_4 h v H_{20}^2}{2} + \frac{\lambda_5 h v H_{20}^2}{2} \\
& + \frac{\lambda_6 h v H_{20}^2}{2} + \frac{\lambda_4 v^2 H_{20}^2}{4} + \frac{\lambda_5 v^2 H_{20}^2}{4} + \frac{\lambda_6 v^2 H_{20}^2}{4} + \frac{\lambda_2 A_{20}^2 H_{20}^2}{4} + \frac{\lambda_{10} A_{30}^2 H_{20}^2}{4} + \frac{\lambda_{11} A_{30}^2 H_{20}^2}{4} \\
& - \frac{\lambda_{12} A_{30}^2 H_{20}^2}{4} + \frac{\lambda_2 H_{20}^4}{8} + \lambda_{12} A_{20} A_{30} H_{20} H_{30} + \frac{\lambda_7 h^2 H_{30}^2}{4} + \frac{\lambda_8 h^2 H_{30}^2}{4} + \frac{\lambda_9 h^2 H_{30}^2}{4} + \frac{\mu_3^2 H_{30}^2}{2} \\
& + \frac{\lambda_7 h v H_{30}^2}{2} + \frac{\lambda_8 h v H_{30}^2}{2} + \frac{\lambda_9 h v H_{30}^2}{2} + \frac{\lambda_7 v^2 H_{30}^2}{4} + \frac{\lambda_8 v^2 H_{30}^2}{4} + \frac{\lambda_9 v^2 H_{30}^2}{4} \\
& + \frac{\lambda_{10} A_{20}^2 H_{30}^2}{4} + \frac{\lambda_{11} A_{20}^2 H_{30}^2}{4} - \frac{\lambda_{12} A_{20}^2 H_{30}^2}{4} + \frac{\lambda_3 A_{30}^2 H_{30}^2}{4} + \frac{\lambda_{10} H_{20}^2 H_{30}^2}{4} + \frac{\lambda_{11} H_{20}^2 H_{30}^2}{4} \\
& + \frac{\lambda_{12} H_{20}^2 H_{30}^2}{4} + \frac{\lambda_3 H_{30}^4}{8} + \frac{\lambda_4 h^2 H_2^- H_2^+}{2} + \mu_2^2 H_2^- H_2^+ + \lambda_4 h v H_2^- H_2^+ + \frac{\lambda_4 v^2 H_2^- H_2^+}{2} \\
& + \frac{\lambda_2 A_{20}^2 H_2^- H_2^+}{2} + \frac{\lambda_{10} A_{30}^2 H_2^- H_2^+}{2} + \frac{\lambda_2 H_{20}^2 H_2^- H_2^+}{2} + \frac{\lambda_{10} H_{30}^2 H_2^- H_2^+}{2} + \frac{\lambda_{11} A_{20} A_{30} H_3^- H_2^+}{2} \\
& + \frac{\lambda_{12} A_{20} A_{30} H_3^- H_2^+}{2} + \frac{i\lambda_{11} A_{30} H_{20} H_3^- H_2^+}{2} - \frac{i\lambda_{12} A_{30} H_{20} H_3^- H_2^+}{2} - \frac{i\lambda_{11} A_{20} H_{30} H_3^- H_2^+}{2} \\
& + \frac{i\lambda_{12} A_{20} H_{30} H_3^- H_2^+}{2} + \frac{\lambda_{11} H_{20} H_{30} H_3^- H_2^+}{2} + \frac{\lambda_{12} H_{20} H_{30} H_3^- H_2^+}{2} + \frac{\lambda_2 (H_2^-)^2 (H_2^+)^2}{2} \\
& + \frac{\lambda_1 2 (H_3^-)^2 (H_2^+)^2}{2} + \frac{\lambda_{11} A_{20} A_{30} H_2^- H_3^+}{2} + \frac{\lambda_{12} A_{20} A_{30} H_2^- H_3^+}{2} - \frac{i\lambda_{11} A_{30} H_{20} H_2^- H_3^+}{2} \\
& + \frac{i\lambda_{12} A_{30} H_{20} H_2^- H_3^+}{2} + \frac{i\lambda_{11} A_{20} H_{30} H_2^- H_3^+}{2} - \frac{i\lambda_{12} A_{20} H_{30} H_2^- H_3^+}{2} + \frac{\lambda_{11} H_{20} H_{30} H_2^- H_3^+}{2} \\
& + \frac{\lambda_{12} H_{20} H_{30} H_2^- H_3^+}{2} + \frac{\lambda_7 h^2 H_3^- H_3^+}{2} + \mu_3^2 H_3^- H_3^+ + \lambda_7 h v H_3^- H_3^+ + \frac{\lambda_7 v^2 H_3^- H_3^+}{2} \\
& + \frac{\lambda_{10} A_{20}^2 H_3^- H_3^+}{2} + \frac{\lambda_3 A_{30}^2 H_3^- H_3^+}{2} + \frac{\lambda_{10} H_{20}^2 H_3^- H_3^+}{2} + \frac{\lambda_3 H_{30}^2 H_3^- H_3^+}{2} \\
& + \lambda_{10} H_2^- H_3^- H_2^+ H_3^+ + \lambda_{11} H_2^- H_3^- H_2^+ H_3^+ + \frac{\lambda_{12} (H_2^-)^2 (H_3^+)^2}{2} + \frac{\lambda_3 (H_3^-)^2 (H_3^+)^2}{2} \tag{67}
\end{aligned}$$

From this potential we can see that there are few terms that are imaginary. Also if we take coefficient $\lambda_{11} = \lambda_{12}$ then we can get rid of these imaginary terms.

We have also tried the potential for two inert plus one Higgs doublet stabilized by different symmetries like $Z_2 \times Z_3$ and $Z_3 \times Z'_3$ but also in these cases, we are getting imaginary terms in the potential.

The part of potential which gives rise to imaginary term in $Z_2 \times Z'_2$ symmetric potential is

$$V = \lambda_{11}(\phi_2^\dagger \phi_3)(\phi_3^\dagger \phi_2) + \frac{\lambda_{12}}{2} [(\phi_2^\dagger \phi_3)^2 + (\phi_3^\dagger \phi_2)^2] \quad (68)$$

So, by making two coefficients same we can get rid off imaginary part. Now consider the potential for $Z_2 \times Z_3$

$$\begin{aligned} V = & \mu_1^2(\phi_1^\dagger \phi_1) + \mu_2^2(\phi_2^\dagger \phi_2) + \mu_3^2(\phi_3^\dagger \phi_3) \\ & + \frac{\lambda_1}{2}(\phi_1^\dagger \phi_1)^2 + \frac{\lambda_2}{2}(\phi_2^\dagger \phi_2)^2 + \frac{\lambda_3}{2}(\phi_3^\dagger \phi_3)^2 + \lambda_4(\phi_1^\dagger \phi_1)(\phi_2^\dagger \phi_2) \\ & + \lambda_5(\phi_1^\dagger \phi_2)(\phi_2^\dagger \phi_1) + \frac{\lambda_6}{2} [(\phi_1^\dagger \phi_2)^2 + (\phi_2^\dagger \phi_1)^2] + \lambda_7(\phi_1^\dagger \phi_1)(\phi_3^\dagger \phi_3) \\ & + \lambda_8(\phi_1^\dagger \phi_3)(\phi_3^\dagger \phi_1) + \lambda_{10}(\phi_2^\dagger \phi_2)(\phi_3^\dagger \phi_3) + \lambda_{11}(\phi_2^\dagger \phi_3)(\phi_3^\dagger \phi_2) \end{aligned} \quad (69)$$

So, in this case we don't have the term that is there in $Z_2 \times Z'_2$ with coefficient λ_{12} so we cannot remove imaginary term. Similarly in $Z_3 \times Z'_3$ we won't get second term due to symmetry conservation. So, in these two cases we are unable to get rid of these imaginary terms by making any two coefficients same as we did in $Z_2 \times Z'_2$ case by making $\lambda_{11} = \lambda_{12}$.

In general, part of potential $[(\phi_2^\dagger \phi_3)(\phi_3^\dagger \phi_2)]$ which gives rise to imaginary term will always be there in any two inert Higgs doublet model stabilised by $Z_n \times Z_m$ symmetry for any integer value of n and m since this is invariant under any unitary transformation.

This term is also present in few papers on inert Higgs doublet model^{[13][14]}.

But later on we realized that there should not be any imaginary term in the potential. However, in order to reduce the parameter we have used $\lambda_{11} = \lambda_{12}$.

10 Positron Excess as a ray of hope for Dark Matter Searches

Positron excess found in cosmic ray by AMS detector could be a possible evidence of existence of dark matter.

10.1 AMS Detector

Alpha Magnetic Spectrometer (AMS-02) is a detector placed at International Space Station (ISS). It is a successor of AMS-01 which was a more simple detector sent to check whether detector concept works in space. AMS-02 is capable of detecting positron, electron, proton and antiproton in cosmic ray and at their energies. It is currently detecting cosmic ray particles in the energy range of 0.5 GeV to 500 GeV^[15]. It is one of the most sophisticated particle physics detectors sent to space. Main aim of AMS is to search for antimatter and prove the existence of dark matter.

10.2 Positron Fraction and Dark Matter

Positron is the antiparticle of electron. Although big bang cosmology suggests that equal amount of matter and antimatter are produced but now our Universe contains only matter with only trace amount of antimatter. It is usually assumed that some asymmetry was processed during early Universe and symmetric part got annihilated so that only asymmetric part remains. Since asymmetry created more matter than antimatter so we are left with only matter. So this trace amount of antimatter (like positron, antiproton etc) present in cosmic ray suggests that there is some mechanism that is producing them along with matter.

Annihilation of dark matter is one such process that can possibly produce electron and positron. Two dark matter annihilate via Higgs h to electron and positron. These excess electrons and positrons can be detected in cosmic ray. But there are other astrophysical sources like pulsars that could produce these excess electrons and positrons. But observation of AMS-02 suggests that positron excess is isotropic^[15] which means that flux is same in all directions. This clearly suggests that this excess is not coming from any astrophysical source like pulsar because flux from an astrophysical source must be in a preferred direction.

Electron flux consists of primary electron, secondary electron and electron produced from decay or annihilation of dark matter whereas positron flux only consists of secondary positron and positron from dark matter. Primary flux is supposed to be produced from supernova remnants whereas secondary flux is produced from the collision of charged particles with cosmic ray. These can be written as^[16]

$$\phi_e^{tot} = \kappa_1 \phi_e^{primary} + \kappa_2 \phi_e^{secondary} + \phi_e^{DM} \quad (70)$$

$$\phi_p^{tot} = \kappa_2 \phi_p^{secondary} + \phi_p^{DM} \quad (71)$$

10.3 Explanation of AMS-02 Data

AMS measures the high energy particles in cosmic ray. Out of 41 billion events analysed, 10 million are identified as electrons and positrons^[15]. Based on these observations, AMS collaboration has plotted the positron fraction versus energy of positron in the energy range of 0.5-500 GeV^[15]. Positron fraction is the ratio of number of positrons divided by total number of positrons plus electrons.

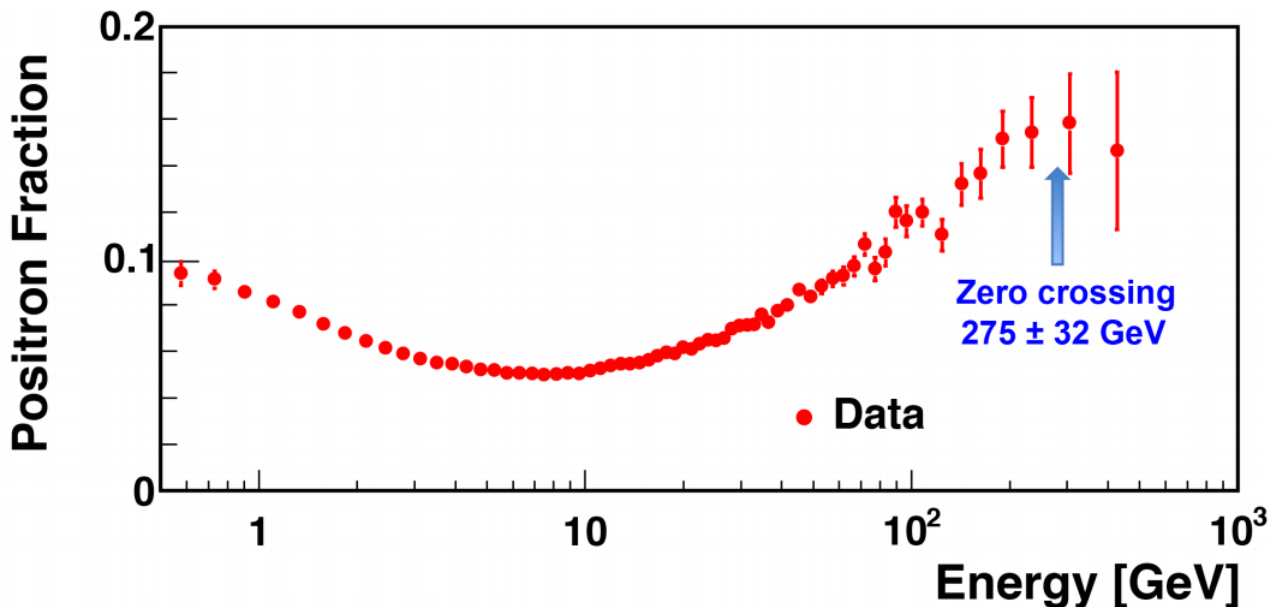


Figure 6: *This figure shows the variation of positron fraction with energy.*

From this figure it is quite evident that there is a rise in positron fraction after 8 GeV. This rise in positron fraction cannot be explained by any cosmic ray collision event. Also it is usually considered that solar modulation can affect this spectra but only at lower energies below 10 GeV. So positron fraction at higher energies is not much affected by solar modulation.

But if we assume that dark matter can annihilate via some annihilation channel to electron and positron then this rise in positron can be explained. There are several dark matter models that are explaining this rise upto certain level of accuracy. Also, it has been proposed in the literature^[16] that if we consider a dark matter model with more than one dark matter candidate then these data can be explained more accurately.

Also, there is one more interesting question arising from this plot. There is a zero crossing point at around 275 ± 32 GeV^[15] which is strange. It is yet an unanswered question why positron flux started decreasing after this

particular energy.

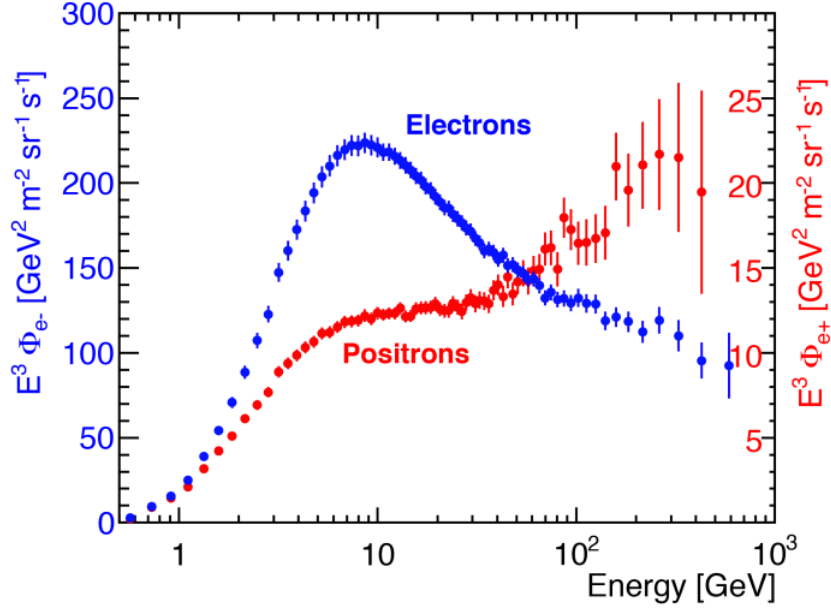


Figure 7: *This figure shows the variation of electron flux (blue points) and positron flux (red points) with energy.*

From this figure we can see that there is a difference between matter and antimatter flux. However it is a bit controversial to say from this figure that there is a difference between matter and antimatter, since scale of electron flux and positron flux in this figure is different and there are certain points where electron flux rises. And even these fluctuations are very small as compared to positron flux but in order to compare these two we have to magnify electron flux ten times. In that case, we can probably observe some similarity between electron and positron flux.

10.4 Formalism

Propagation of positron inside galaxy can be explained by a diffusion equation. While moving in galaxy it loses energy as synchrotron radiation during its propagation in interstellar magnetic field. It may also lose energy through inverse Compton scattering while moving through CMB or through diffused starlight.

Time rate of change in number of positron per unit energy is given as^[17]

$$\frac{\partial}{\partial t} \frac{dn_{e^+}}{dE_{e^+}} = \vec{\nabla} \cdot \left[K(E_{e^+}, \vec{x}) \vec{\nabla} \frac{dn_{e^+}}{dE_{e^+}} \right] + \frac{\partial}{\partial E_{e^+}} \left[b(E_{e^+}, \vec{x}) \frac{dn_{e^+}}{dE_{e^+}} \right] + Q(E_{e^+}, \vec{x}) \quad (72)$$

where $b(E_{e^+}, \vec{x})$ is the rate at which positron loses energy and $K(E_{e^+}, \vec{x})$ is diffusion constant. The term $Q(E_{e^+}, \vec{x})$ takes care of new positron coming from dark matter annihilation and injected into the spectrum (in $cm^{-3}s^{-1}$). On solving this transport equation we can get the positron number density per unit energy $\frac{dn_{e^+}}{dE_{e^+}}$. This positron number density is related to flux by the formula,

$$\frac{d\phi}{dE_{e^+}} = \frac{\beta c}{4\pi} \frac{dn_{e^+}}{dE_{e^+}} \quad (73)$$

This is important because positron fraction is given as

$$\frac{e^+}{e^+ + e^-} = \frac{\frac{d\phi}{dE_{e^+}}}{\frac{d\phi}{dE_{e^+}} + \frac{d\phi}{dE_{e^-}}} \quad (74)$$

In order to match with the experimental data we can make a plot of positron flux versus energy for any given model. The term which depends on model is the source term $Q(E_{e^+}, \vec{x})$.

$$Q(E_{e^+}, \vec{x}) = \Sigma_f \langle \sigma_{ann} v \rangle_{tot} \cdot BR_f \cdot \frac{dN_f}{dE} \cdot \frac{\rho_{DM}^2(\vec{x})}{M_{DM}^2} \quad (75)$$

So for a given dark matter model we can take annihilation cross section and mass of dark matter and branching fraction to different annihilation channels and use in equation (75) to get source term. We can further use the latter in equation (72) to get positron number density per unit energy.

11 Gamma Ray Excess from Galactic Center

After the results of Fermi Gamma Ray Space Telescope (FGST) revealed the gamma ray excess at the galactic center, there has been a great deal of discussion among particle and astrophysics community about the origin of this excess.

11.1 Fermi Gamma Ray Space Telescope

FGST is a space based gamma ray observatory. There are two important instruments onboard FGST, a Large Area Telescope (LAT) and a Gamma Ray Burst Monitor (GBM). LAT is a gamma ray detector that can detect photons within the energy range of 20 MeV to 300 GeV.

Fermi LAT has first observed the bubble shaped gamma ray lobes at the galactic center extending about 25000 light year (1 light year = 9.46×10^{15} meter) above and below the galactic plane.

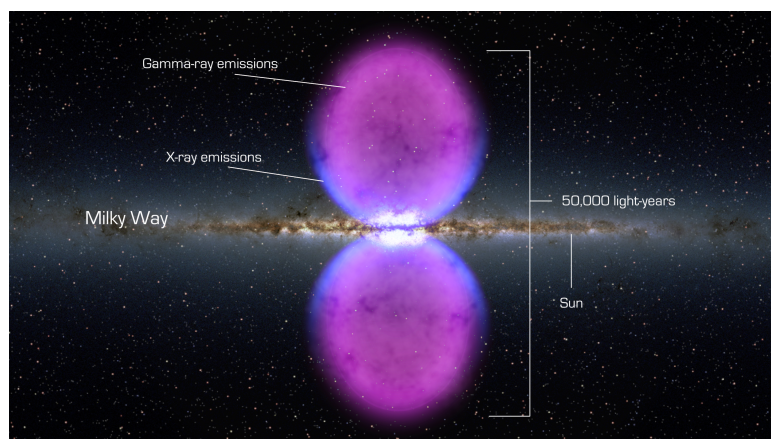


Figure 8: *This figure shows the Fermi bubble extending 25000 light year above and below galactic plane.*

11.2 Gamma Ray Excess and Dark Matter

Many efforts have been made to describe this gamma ray excess from known sources. But it has been found that it is not possible to explain this excess completely from known sources. Like in [18] two year data of Fermi Gamma Ray Space Telescope has been analyzed within 10° around the galactic center. It was found that the spectrum between 1.25° to 10° can be explained with the known source of gamma ray. But the spectrum within 1.25° deviates from what is expected^[18].

However if we consider a scenario where dark matter annihilation or decay takes at the galactic center resulting in production of gamma ray then this excess in gamma ray can be explained for some particular mass range and annihilation cross section of dark matter.

Galactic center is important location for such kind of dark matter annihilation processes since gravity of supermassive black hole can trap dark matter in its proximity and hence they can annihilate.

11.3 Formalism

For any given dark matter model we can calculate the flux of photons produced by annihilation or decay of dark matter.

The differential flux of gamma ray produced by annihilation or decay of dark matter in a particular angular direction can be calculated based on simple logic.

For any dark matter annihilation or decay process, flux ϕ of product is proportional to the number of annihilation or decay taking place per unit time per unit volume^[18]. So for annihilation,

$$\phi \propto \sigma v n^2(r)$$

Also,

$$n(r) = \frac{\rho}{m_{DM}}$$

So

$$\phi \propto \sigma v \frac{\rho^2(r)}{m_{DM}^2}$$

where $n(r)$ is number density of dark matter and $\rho(r)$ is mass density of dark matter. Here σv is annihilation cross section times velocity and r is the distance from galactic center. Flux will also depend upon the number of secondary particles produced per unit energy per annihilation ($\frac{dN_i}{dE}$) for a particular species i . We can find total flux in a given energy range and in a particular range of solid angle by integrating the density square term along a line of sight joining solar location to the galactic center. So total flux is given as^[19]

$$\frac{d\phi_\gamma}{d\Omega dE} = \frac{1}{2} \frac{r_\odot}{4\pi} \left(\frac{\rho_\odot}{M_{DM}} \right)^2 \Sigma_f \langle \sigma v \rangle_f \frac{dN_\gamma^f}{dE} \int_{l.o.s} \frac{ds}{r_\odot} \left(\frac{\rho(r(s, \theta))}{\rho_\odot} \right)^2 \quad (76)$$

Now from this equation we can separate particle physics dependent part and halo profile part.

So, on separating we get

$$\frac{d\phi_\gamma}{d\Omega dE} = \frac{1}{2} \frac{r_\odot}{4\pi} \left(\frac{\rho_\odot}{M_{DM}} \right)^2 J \Sigma_f \langle \sigma v \rangle_f \frac{dN_\gamma^f}{dE} \quad (77)$$

Where J is halo profile dependent part and given as

$$J = \int_{l.o.s} \frac{ds}{r_\odot} \left(\frac{\rho(r(s, \theta))}{\rho_\odot} \right)^2 \quad (78)$$

For decay

$$\frac{d\phi_\gamma}{d\Omega dE} = \frac{1}{2} \frac{r_\odot}{4\pi} \left(\frac{\rho_\odot}{M_{DM}} \right) J \Sigma_f \Gamma_f \frac{dN_\gamma^f}{dE} \quad (79)$$

where

$$J = \int_{l.o.s} \frac{ds}{r_\odot} \left(\frac{\rho(r(s, \theta))}{\rho_\odot} \right) \quad (80)$$

Here the center of coordinate system is considered at the galactic center and coordinate r is explained in terms of s and θ .

Let r_{\odot} be the distance from galactic center to our Earth and s is the distance along line of sight from Earth. Here θ is the angle between the line of sight and the line joining earth to center of galaxy. Distance of any point on the halo from galactic center is given as $r(s, \theta) = (r_{\odot}^2 + s^2 - 2r_{\odot}s\cos\theta)^{1/2}$.

Now, in order to get integrated flux in a given solid angle $\Delta\Omega$ we have to replace J by averaging J over $\Delta\Omega$. So average J (\bar{J}) is given as

$$\bar{J} = \frac{\int_{\Delta\Omega} J d\Omega}{\Delta\Omega} \quad (81)$$

where

$$\Delta\Omega = 2\pi \int_0^{\theta_{max}} d\theta \sin\theta \quad (82)$$

So

$$\bar{J} = \frac{2\pi}{\Delta\Omega} \int d\theta \sin\theta J(\theta) \quad (83)$$

11.3.1 Dark Matter Halo Profile

Distribution of dark matter around galactic center is determined by its halo profile. Various simulation studies of galaxy formation and their comparison with observation data give different halo profiles.

Some of the most widely accepted halo profiles are Navarro-Frenk-White (NFW)^[21] halo profile and Moore^[22] profile.

Dark matter density at a given location from galactic center is given as^[20]

$$\rho(r) = \rho_0 \left[\frac{r_{\odot}}{r} \right]^{\gamma} \left[\frac{1 + \left[\frac{r_{\odot}}{a} \right]^{\alpha}}{1 + \left[\frac{r}{a} \right]^{\alpha}} \right]^{\left(\frac{\beta-\gamma}{\alpha} \right)} \quad (84)$$

where for NFW profile $\alpha=1$, $\beta=3$, $\gamma=1$ and $a = 20$ kpc and for Moore profile $\alpha=1.5$, $\beta=3$, $\gamma=1.5$ and $a = 28$ kpc.

12 Experimental Results

This model is satisfying the result for relic density of dark matter $\Omega_{DM}h^2 = 0.116$ as estimated by various cosmic microwave background radiation (CMBR) experiments. Both dark matter candidates contribute to the total relic density as follows:

$$m_{H_{20}} = 552 \text{ GeV}$$

$$m_{A_{20}} = 557 \text{ GeV}$$

$$m_{H_2^+} = 562 \text{ GeV}$$

$$H_{20}H_{20}h \text{ coupling } \left(\frac{\lambda_4+\lambda_5+\lambda_6}{2}\right) = 0.001$$

$$m_{H_{30}} = 500 \text{ GeV}$$

$$m_{A_{30}} = 505 \text{ GeV}$$

$$m_{H_3^+} = 501 \text{ GeV}$$

$$H_{30}H_{30}h \text{ coupling } \left(\frac{\lambda_7+\lambda_8+\lambda_9}{2}\right) = 0.001$$

For these sets of parameters the contributions of H_{20} and H_{30} are calculated to be 21% and 79% respectively of total $\Omega_{DM}h^2 = 0.116$.

13 Conclusion

In this report, we have tried to construct basic understanding of what dark matter is, what are the evidences of dark matter and its detection methods. We have done some literature survey on asymmetric dark matter models and multi-component dark matter model. Based on that we are trying to construct a model for two inert doublet added to standard model Higgs doublet. We have considered a potential stabilized by discrete symmetry $Z_2 \times Z'_2$. Here one inert doublet is odd under Z_2 and other inert doublet odd under Z'_2 . We have calculated mass term of various components of the doublet and the criteria for boundedness of the potential. We have also shown that for a given parameter space this model is satisfying the relic density constraint.

We have also studied the formalism for explaining certain experimental observations like gamma ray excess found at the galactic center and positron excess found in the cosmic rays from a given dark matter model.

Based on studies of formalism for gamma ray excess and positron excess we can make plot for flux versus energy for this model and try to relate it with the experimental observations.

A model with two dark matter candidates is better as compared to models with one dark matter candidate. Because in models for two dark matter candidates, we can have more diverse phenomenology and we can explain some of the constraints put up by various experiments more accurately as compared to the models with one dark matter candidate.

14 References

1. Murayama H. (2007), Physics Beyond the Standard Model and Dark Matter, arxiv: 0704.2276.
2. Petraki K. and Volkas R. R. (2013), Review of Asymmetric Dark Matter, *Int. J. Mod. Phys. A*28 (2013) 1330028, (DOI: 10.1142/S0217751X13300287).
3. Bernabei R. *et al.* (2008), First results from DAMA/LIBRA and the combined results with DAMA/NaI, *Eur. Phys. J. C*56 (2008) 333-355, (DOI: 10.1140/epjc/s10052-008-0662-y).
4. Aalseth C. E. *et al.* (2011), Results from a Search for Light-Mass Dark Matter with a P-type Point Contact Germanium Detector, *Phys. Rev. Lett.* 106 (2011) 131301, (DOI: 10.1103/PhysRevLett.106.131301).
5. Aalseth C. E. *et al.* (2011), Search for an Annual Modulation in a P-type Point Contact Germanium Dark Matter Detector, *Phys. Rev. Lett.* 107 (2011) 141301, (DOI: 10.1103/PhysRevLett.107.141301).
6. Angloher G., Bauer M., Bavykina I., Bento A., Bucci C., Ciemniak C., Deuter G., Feilitzsch F. V., Hauff D., Huff P. *et al.* (2012), Results from 730 kg days of the CRESST-II Dark Matter Search, *Eur. Phys. J. C*72 (2012) 1971, (DOI: 10.1140/epjc/s10052-012-1971-8).
7. Agnese R. *et al.* (2013), Silicon Detector Dark Matter Results from the Final Exposure of CDMS II, *Phys. Rev. Lett.* 111 (2013) 25, 251301, (DOI: 10.1103/PhysRevLett.111.251301).
8. Hinshaw G. *et al.* (2012), Nine-Year Wilkinson Microwave Anisotropy Probe (WMAP) Observations: Cosmological Parameter Results, *Astrophys. J. Suppl.* 208 (2013) 19, (DOI: 10.1088/0067-0049/208/2/19).
9. Ade P.A.R. *et al.* (2013), Planck 2013 Result. XVI. Cosmological Parameters, *Astron. Astrophys.* 571 (2014) A16, (DOI: 10.1051/0004-6361/201321591).

10. Finkbeiner D. P. and Weiner N. (2007), Exciting Dark Matter and the INTEGRAL/SPI 511 keV signal, *Phys.Rev. D* 76 (2007) 083519, (DOI: 10.1103/PhysRevD.76.083519).
11. Modak K. P., Majumdar D. and Rakshit S. (2015), A Possible Explanation of Low Energy γ -ray Excess From Galactic Center and Fermi Bubble by a Dark Matter Model with Two Real Scalars, *JCAP* 1503 (2015) 011, (DOI: 10.1088/1475-7516/2015/03/011).
12. Chakraborty J., Konar P. and Mondal T. (2014), Copositivity Criteria and Boundedness of Scalar Potential, *Phys. Rev. D* 89 (2014) 9, 095008, (DOI: 10.1103/PhysRevD.89.095008).
13. Keus V., King S. F. and Moretti S. (2014), Phenomenology of the Inert (2+1) and (4+2) Higgs Doublet Models, *Phys. Rev. D* 90 (2014) 7, 075015, (DOI: 10.1103/PhysRevD.90.075015).
14. Keus V., King S. F. and Moretti S. (2014), Dark Matter with Two Inert Doublet Plus One Higgs Doublet, *JHEP* 1411 (2014) 016, (DOI: 10.1007/JHEP11(2014)016).
15. New result from Alpha Magnetic Spectrometer on International Space Station, [http://www.ams.nasa.gov/Documents/AMS Publications/ams new results - 18.09.2014.pdf](http://www.ams.nasa.gov/Documents/AMS%20Publications/ams%20new%20results%20-%2018.09.2014.pdf).
16. Geng C. Q., Huang D. and Lai C. (2015), Revisiting Multicomponent Dark Matter with new AMS-02 Data, *Phys. Rev. D* 91 (2015) 9, 095006, (DOI: 10.1103/PhysRevD.91.095006).
17. Nezri E., Tytgat M. H. G. and Vertongen G. (2009), e^+ and \bar{p} from inert doublet model Dark Matter, *JCAP* 0904 (2009) 014, (DOI: 10.1088/1475-7516/2009/04/014).
18. Hooper D. and Goodenough L. (2011), Dark Matter Annihilation in Galactic Center as seen by Fermi Gamma Ray Space Telescope, *Phys. Lett.*

B697 (2011) 412-428, (DOI: 10.1016/j.physletb.2011.02.029).

19. Cirelli M., Corcella G., Hektor A., Hutsi G., Kadastik M., Panci P., Raidal M., Sala F. and Strumia A. (2011, 2012), PPPC 4 DM ID: A Poor Particle Physicist Cookbook for Dark Matter Indirect Detection, JCAP 1103 (2011) 051, JCAP 1210 (2012) E01, (DOI: 10.1088/1475-7516/2011/03/051), (DOI: 10.1088/1475-7516/2012/10/E01).

20. Majumdar D., Dark Matter An Introduction, CRC Press, ISBN- 10.1088/1475-7516/2011/03/051.

21. Navarro J. F., Frenk C.S. and White S.D.M. (1996), The Structure of Cold Dark Matter Halos, *Astrophys. J.* 462: 563-575, 1996, (DOI: 10.1086/177173).

22. Moore B., Ghigna S., Governato F., Lake G., Quinn T., Stadel J. and Tozzi P. (1999), Dark Matter Substructure in Galactic Halo, *Astrophys. J.* 524: L19-L22, 1999, (DOI: 10.1086/312287).